

A rapid transition from ice covered CO₂-rich waters to a biologically mediated CO₂ sink in the eastern Weddell Gyre

D. C. E. Bakker¹, M. Hoppema², M. Schröder², W. Geibert^{2,*}, and H. J. W. de Baar³

¹School of Environmental Sciences, University of East Anglia, Norwich, UK

²Alfred Wegener Institute for Polar and Marine Research, Bremerhaven, Germany

³Royal Netherlands Institute for Sea Research, Texel, The Netherlands

* now at: Earth Science, School of Geosciences, University of Edinburgh, Edinburgh, UK

Received: 18 February 2008 – Published in Biogeosciences Discuss.: 25 March 2008

Revised: 26 August 2008 – Accepted: 26 August 2008 – Published: 30 September 2008

Abstract. Circumpolar Deep Water (CDW), locally called Warm Deep Water (WDW), enters the Weddell Gyre in the southeast, roughly at 25° E to 30° E. In December 2002 and January 2003 we studied the effect of entrainment of WDW on the fugacity of carbon dioxide (fCO₂) and dissolved inorganic carbon (DIC) in Weddell Sea surface waters. Ultimately the fCO₂ difference across the sea surface drives air-sea fluxes of CO₂. Deep CTD sections and surface transects of fCO₂ were made along the Prime Meridian, a northwest-southeast section, and along 17° E to 23° E during cruise ANT XX/2 on FS *Polarstern*. Upward movement and entrainment of WDW into the winter mixed layer had significantly increased DIC and fCO₂ below the sea ice along 0° W and 17° E to 23° E, notably in the southern Weddell Gyre. Nonetheless, the ice cover largely prevented outgassing of CO₂ to the atmosphere. During and upon melting of the ice, biological activity rapidly reduced surface water fCO₂ by up to 100 μatm, thus creating a sink for atmospheric CO₂. Despite the tendency of the surfacing WDW to cause CO₂ supersaturation, the Weddell Gyre may well be a CO₂ sink on an annual basis due to this effective mechanism involving ice cover and ensuing biological fCO₂ reduction. Dissolution of calcium carbonate (CaCO₃) in melting sea ice may play a minor role in this rapid reduction of surface water fCO₂.

(Sabine et al., 2004; McNeil et al., 2007). Recent observations and modelling suggest that the Southern Ocean is particularly sensitive to changes, be they anthropogenic or not (Stephens and Keeling, 2000; Hoppema, 2004; Lenton and Matear, 2007; Le Quéré et al., 2007; Lovenduski et al., 2007; Zickfeld et al., 2007). Upwelling of CO₂-enriched deep water and its long-term trends play the major role in all these analyses.

The Weddell Gyre is an elongated, mainly wind-driven, cyclonic gyre in the Atlantic sector of the Southern Ocean, south of the Antarctic Circumpolar Current (ACC). Water flows westwards in the southern limb and eastwards in the northern limb of the gyre (Fig. 1). Due to its divergent nature, Ekman pumping causes major upward transport of subsurface water in the gyre's interior. Formation of deep and bottom water occurs in the southern and western parts of the gyre (e.g. Carmack and Foster, 1975; Gordon et al., 1993); dense water originating here is found in most of the Southern Hemisphere as Antarctic Bottom Water (AABW). Surface water of the gyre is exchanged with the adjacent ACC along all of its northern and eastern boundaries. Subsurface water is supplied by the ACC, where it is swept into the Weddell Gyre at its eastern boundary, i.e. 25° E to 30° E (Deacon, 1979; Gouretski and Danilov, 1993; Schröder and Fahrbach, 1999). There may be another subsurface water supply near 20° W (Bagriantsev et al., 1989). This subsurface water, known as Circumpolar Deep Water (CDW), but locally called Warm Deep Water (WDW), is recognized by its temperature maximum (T_{max}) just underneath the pycnocline. The highest T_{max} values are found in the southeastern Weddell Gyre, indicating that that region is the main recipient of CDW source water (Deacon, 1979; Gouretski and Danilov, 1993). On its course through the gyre, the T_{max} is attenuated by mixing with waters above and below. As a result the temperature

1 Introduction

The Southern Ocean plays a pivotal role in the global carbon cycle. A considerable part of the global oceanic uptake of anthropogenic carbon dioxide (CO₂) occurs in this vast region



Correspondence to: D. C. E. Bakker
(d.bakker@uea.ac.uk)

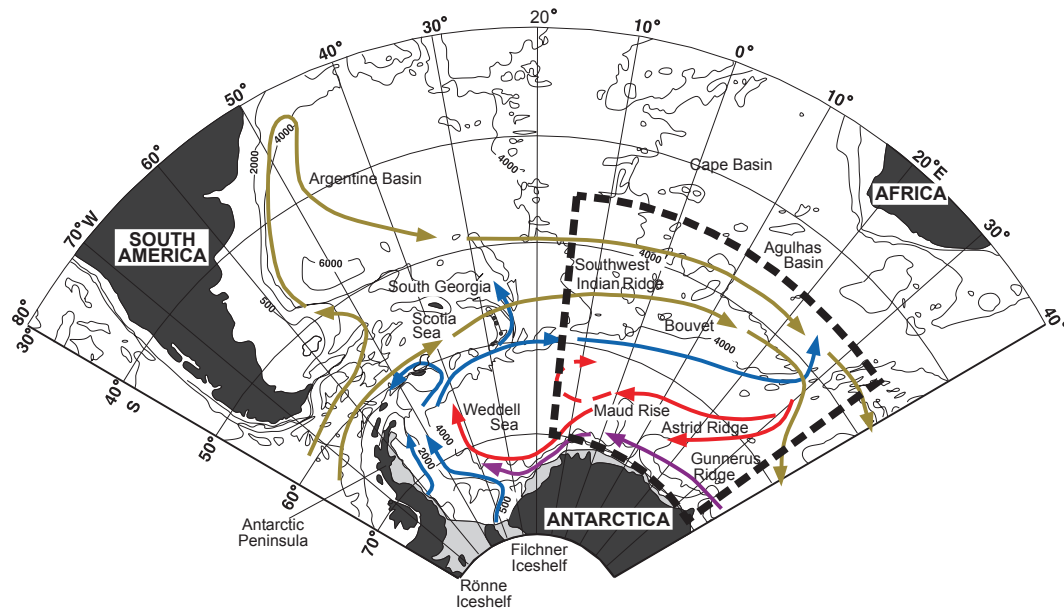


Fig. 1. Map of the Weddell Sea with schematically the deep inflow of Circumpolar Deep Water (CDW) (red) at 25° E to 30° E, the Antarctic Coastal Current (purple), and the formation and outflow of Weddell Sea Bottom Water and Antarctic Bottom Water (blue). The Antarctic Circumpolar Current (ACC) is in green. The research area is within the dashed frame.

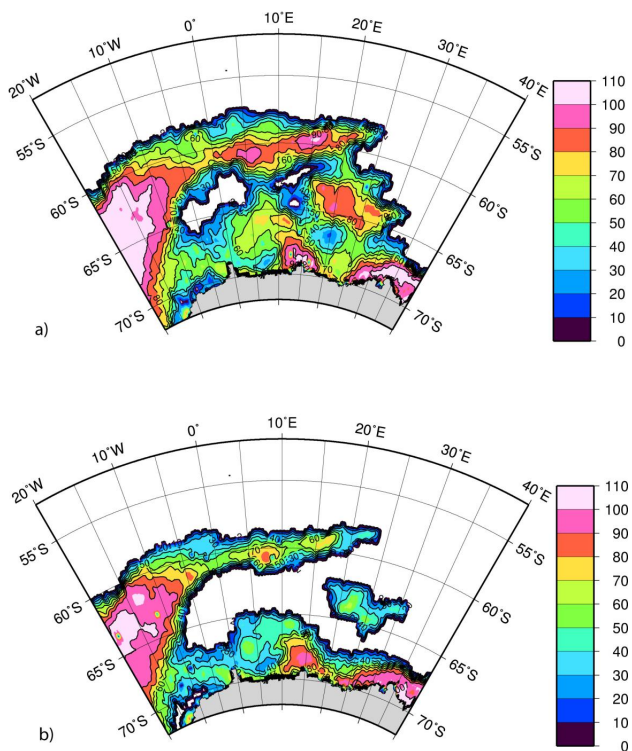


Fig. 2. Maps of the distribution of sea ice (%) in the central and eastern Weddell Gyre for (a) 17 and (b) 24 December 2002 (data from Comiso, 1999; updated 2007).

of the T_{\max} in the southern limb is higher than in the northern limb of the gyre. The T_{\max} is accompanied by maxima of salinity, dissolved inorganic carbon (DIC), and nutrients and by an oxygen minimum (Whitworth and Nowlin, 1987; Hoppema et al., 1997), although the exact depths of the extremes vary and may not be identical.

Seasonal ice coverage is a prominent feature of the Weddell Gyre. In the far west perennial ice is found, while towards the east the vast ice field disappears rapidly in late spring and early summer. Two stages of ice disappearance in the central and eastern gyre are depicted for December 2002 (Fig. 2). By 17 December a transient polynya had formed within the melting ice pack northwest of Maud Rise (Fig. 2a), in a region, which has often been associated with ice melting events and polynyas (e.g. Martinson et al., 1981; Muench et al., 2001). On 24 December 2002, an ice-free area from the east had combined with the initial polynya. Seasonal ice coverage strongly impacts on the cycling of chemical species and biological processes. For example, chlorofluorocarbons (CFCs) and oxygen (O_2) are strongly undersaturated, and CO_2 is oversaturated in ice-covered Weddell Gyre surface waters relative to their atmospheric contents (Gordon et al., 1984; Weiss et al., 1992; Bakker et al., 1997; Klatt et al., 2002), indicating that ice caps the water column, thus hindering air-sea gas exchange.

It has long been suggested that calcium carbonate ($CaCO_3$) precipitates along brine channels in sea ice (Jones and Coote, 1981; Papadimitriou et al., 2004, 2007; Rysgaard et al., 2007). Recently, Dieckmann et al. (2008) detected ikaite, a hydrated $CaCO_3$ mineral ($CaCO_3 \cdot 6H_2O$), in sea ice

from the Weddell Sea. The ikaite was found in sea ice of different types, ranging from 0.25 m thick newly formed Nilas ice to 2.25 m thick multi-year ice. The precipitation of CaCO₃ in sea ice reduces alkalinity and DIC, while increasing fCO₂ (fugacity of CO₂) in the brine. Any brine escaping from the ice would transfer these CO₂ characteristics to the winter mixed layer. During and upon ice melt, any CaCO₃ mineral dissolving in the melting ice or in the surface mixed layer would increase surface water alkalinity and DIC and decrease its fCO₂.

The southeastern Weddell Gyre appears to be vital for exchange processes with the ACC and for preconditioning water masses for their course through the Weddell Gyre. It is a highly dynamical and variable region with many eddies resulting from interactions of the ACC with topography (Gouretski and Danilov, 1993). Local deep-sea promontories, like Astrid Ridge and Maud Rise (Fig. 1), promote vertical mixing (Muench et al., 2001). Upward movement of the newly arriving CDW may well enhance vertical transport (Geibert et al., 2002). The relatively early break-up of the sea ice in the eastern Weddell Gyre (Fig. 2) may be related to the region's dynamic hydrography.

With major interaction between surface waters and CDW, the eastern Weddell Gyre is likely to be important from a biogeochemical point of view, but little is known about it. In spring the partial pressure of CO₂ (pCO₂) in surface water varied strongly with both over- and undersaturation relative to atmospheric CO₂ north of 60° S (Bakker et al., 1999), while in autumn surface water pCO₂ was undersaturated (Hoppema et al., 2000). Sparse chlorophyll and photosynthetic oxygen production data in December suggest low biological activity compared to adjacent regions (Odate et al., 2002). Satellite pigment data also point to low biological production (Sullivan et al., 1993; Moore and Abbott, 2000), while carbon export production is modelled to be among the lowest of the Southern Ocean (Schlitzer, 2002). By contrast, modelled opal export production is relatively high (Usbeck, 1999) and high densities of certain whales have been found in the eastern Weddell Gyre (Tynan, 1998).

Thus, a biogeochemical study of the eastern Weddell Gyre is appropriate. We visited the eastern and central Weddell Gyre, as the ice pack was opening up in late spring and early summer, with the aim to assess the processes controlling surface layer carbon chemistry below the sea ice and upon the retreat of the sea ice. Our hypothesis is that both upwelling of WDW and ice cover exert a significant influence on the partial pressure of CO₂ and the DIC concentration in surface waters. In addition, we test whether the observations agree with the theory of the conversion of a pre-industrial CO₂ source to a present-day annual CO₂ sink in the Weddell Gyre (Hoppema, 2004). Furthermore, we look for evidence supporting the hypothesis of reduced ventilation of CO₂-rich, upwelled water by extensive sea ice coverage in the glacial Southern Ocean (Stephens and Keeling, 2000).

2 Methods

Inorganic carbon data were collected during cruise ANT XX/2 with the German ice breaker FS *Polarstern* starting and ending in Cape Town at 24 November 2002 and 23 January 2003, respectively (Fütterer and Kattner, 2005). The ship made deep sections with stations at 0.5° latitude spacing along the Prime Meridian, along a northwest-southeast cross-transect and along 17° E to 23° E in the Weddell Gyre (Figs. 1 and 3). High resolution vertical profiles of potential temperature and salinity were obtained during the downcasts of the ship's CTD (conductivity, temperature, depth) (type Seabird 911+), while samples for DIC and other biogeochemical parameters were taken from the CTD rosette during the upward casts. Atmospheric pressure, sea surface temperature and salinity were measured by the ship's sensors. While the ship was sailing, ice observations were made at almost hourly intervals from the bridge from 4 December 2002 to 3 January 2003, following the protocols by Worby et al. (1999).

The fugacity of CO₂ was determined quasi-continuously in surface water and marine air from the sailing ship. Water was drawn from about 10 m depth at the keel of the ship, while air was sampled from the crow's nest. Correction of the partial pressure for non-ideal behaviour of CO₂ gas provides the fugacity of CO₂. The measurements were performed with an automated sampling system based on a Li-COR 6262 infrared gas analyzer and designed after Wanninkhof and Thoning (1993). Such a system has been used before on *Polarstern* (e.g. Hoppema et al., 2000; Bellerby et al., 2004). Every three hours the measurements were calibrated by two out of three calibration gases, bracketing surface water fCO₂. The calibration gases of 250.53, 374.36, and 453.65 μmol CO₂ mol⁻¹ had been calibrated to NOAA gas standards prior to the cruise. Warming of the water between the seawater intake and the equilibrator ranged from 0.43°C in subantarctic waters to 0.72°C near sea ice (standard deviation of 0.2°C for 60 000 data points).

The DIC concentration (the sum of all dissolved inorganic carbon species) was determined by coulometry with two instruments. The samples were stored cold and in the dark prior to analysis, but were not poisoned. Almost all samples were analysed within 6 h of collection. Analysis was complete within 24 h. Surface water fCO₂ changes due to in situ biological activity were 1.0 to 3.4 μatm d⁻¹ in optimal light conditions (see Results section), which corresponds to DIC changes of 0.7 to 2.4 μmol kg⁻¹ d⁻¹. Although the absence of poisoning may thus cause a significant error, this worst case will not have occurred, because of sample storage in the dark and rapid analysis. Almost all DIC measurements were performed in triplicate from one sample bottle, which enabled us to discard outliers. Certified reference material (CRM) of batch 53 (Dickson et al., 2007) was used for each CTD cast and for each coulometric cell. Because of instrumental problems, we estimate the precision as ± 1.8 μmol kg⁻¹ (being the standard deviation σ of all

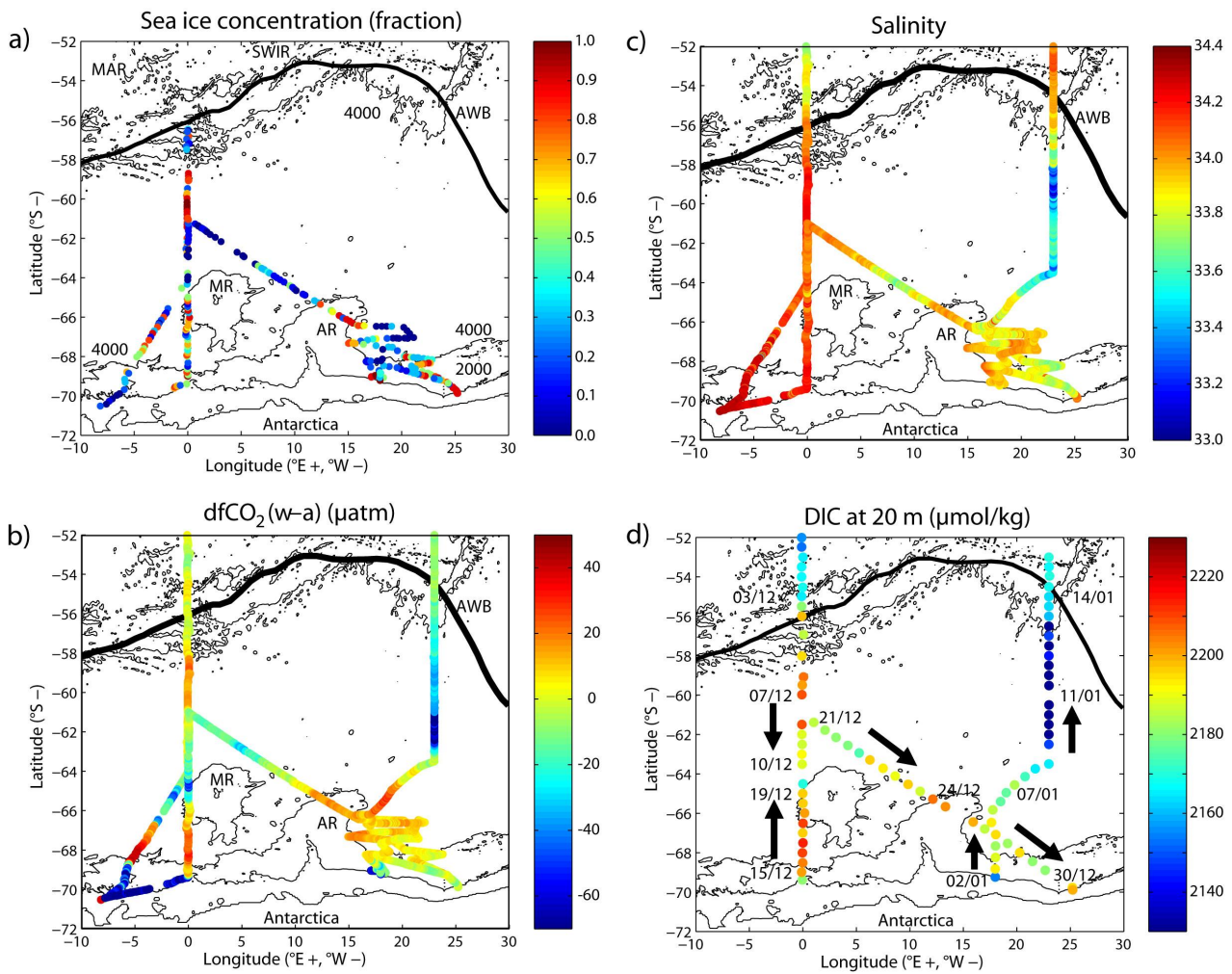


Fig. 3. (a) Sea ice concentration (fraction), (b) the difference of $f\text{CO}_2$ between surface water and marine air, $\Delta f\text{CO}_2(w-a)$, (c) salinity, and (d) DIC at 20 m depth with the timing of the sampling along the cruise track in December 2002 and January 2003. The Antarctic coast line (ETOPO 5, 1988) and depth contours at 2000 m and 4000 m (Smith and Sandwell, 1997, version 8.2) have been indicated. The average position of the ACC-Weddell Boundary (AWB) is given (thick black line) (Orsi et al., 1995). Topographic features are Maud Rise (MR) and Astrid Ridge (AR).

CRMs) and the accuracy as $\pm 2.5 \mu\text{mol kg}^{-1}$, which is less than during previous cruises where the same equipment was used.

Samples for DIC were taken at depths of 20, 50, 100 m and below with occasional samples from 10 and 75 m depth. Here DIC at 20 m depth is taken as the best available proxy for DIC in surface waters. The DIC concentration at 20 m depth exceeded that at 10 m by $3.0 \mu\text{mol kg}^{-1}$ along 0°W (σ of $5.0 \mu\text{mol kg}^{-1}$, n of 8) and by $7.7 \mu\text{mol kg}^{-1}$ along 17°E to 23°E (σ of $5.9 \mu\text{mol kg}^{-1}$, n of 13) at stations where both depths were sampled. The higher offset in the east presumably reflects the progression from spring to summer.

Surface water $f\text{CO}_2$ was co-located to CTD casts by taking the average $f\text{CO}_2$ determined within 20 min (or in a few cases

within 30 min, 60 min or 120 min) of the CTD returning to the surface. Total alkalinity (TA) has been calculated from DIC at 10 m and 20 m depth and $f\text{CO}_2$ at 10 m depth with the constants of Mehrbach et al. (1973), as revised by Dickson and Millero (1987). Such calculations provide alkalinity with an accuracy of $3.4 \mu\text{mol kg}^{-1}$ for accuracies of $2 \mu\text{mol kg}^{-1}$ for DIC and $2 \mu\text{atm}$ for $f\text{CO}_2$ (Millero, 1995). The use of DIC from 20 m depth for a given $f\text{CO}_2$ value at 10 m depth resulted in an overestimation of TA at 20 m by $2.8 \mu\text{mol kg}^{-1}$ (σ of $4.8 \mu\text{mol kg}^{-1}$) and $5.2 \mu\text{mol kg}^{-1}$ (σ of $7.5 \mu\text{mol kg}^{-1}$) for 0°W and $17\text{--}23^\circ \text{E}$, respectively.

Near-surface DIC and calculated alkalinity (TA) were normalised to a salinity of 34.2 with the traditional approach ($\text{TA}_{34.2}$ and $\text{DIC}_{34.2}$) by multiplication with salinity 34.2 and division by the in situ salinity. Friis et al. (2003; also K. Friis,

personal communication) highlight problems with the traditional normalisation of alkalinity and DIC. In our case the salinity correction was generally less than 0.5 units with only higher values of up to 1.5 units at 59° S 23° E, thus we do not expect large offsets with the traditional approach.

3 Results

3.1 Sea ice cover and surface water CO₂ parameters

The ship first reached the ice edge at 4 December 2002 on the Prime Meridian at 56.5° S, roughly on the northern boundary of the Weddell Gyre (Fig. 3a). Over the next month FS *Polarstern* sailed through fully ice covered waters, areas with melting sea ice and open water in the Weddell Gyre. Two maps of the satellite-derived ice fraction give a picture of the rapidly disappearing ice pack and of high spatial variability between ice-covered waters and open water in December 2002 (Fig. 2). The ship finally left the ice pack in the eastern Weddell Gyre on 68.2° S 18.1° E on 3 January 2003 (Fig. 3a).

The fCO₂ difference between surface water and air, ΔfCO₂(w–a), varied from strong supersaturation to strong undersaturation along the cruise track in the Weddell Gyre (Fig. 3b). The distribution of DIC at 20 m depth showed a similar large spatial variability with a good correspondence between DIC and ΔfCO₂(w–a) (Fig. 3d). On the Prime Meridian the ice coverage, ΔfCO₂(w–a) and DIC were high in the northern Weddell Gyre. Significantly lower ΔfCO₂(w–a) and DIC were observed in a newly forming polynya at 62° S to 65° S, northwest of Maud Rise. A repeat visit to 61° S to 64° S along 0° W highlights the reduction of surface water fCO₂ during sea ice melt over an 11 day period in this polynya (Fig. 4). On 8 to 10 December a significant fraction of the ice cover had disappeared, the remaining sea ice was melting rapidly, surface water fCO₂ was close to the atmospheric value and the sea surface temperature was –1.8 to –1.7°C. Eleven days later sea ice had disappeared along most of the section, surface water fCO₂ had been reduced by 10 to 25 μatm and the water had warmed by up to 0.8°C. This translates into a rate of surface water fCO₂ decrease of 1.0 to 2.5 μatm d^{–1} or 1.0 to 3.4 μatm d^{–1} upon correction to a constant temperature. The highest rates were found at 63° S to 64° S, where the ice melted first and a phytoplankton bloom was developing. These maximum rates were only just below the fCO₂ decrease of 3.8 μatm d^{–1} by phytoplankton growing at a maximum growth rate in an iron-fertilised algal bloom at 61° S 139° W (Bakker et al., 2001). This suggests that iron was abundant and not limiting for phytoplankton growth in the Weddell surface layer during ice melt.

South of the polynya ΔfCO₂(w–a) and DIC were high in an area with thick ice cover and melting sea ice (Figs. 2a and 3). Along the Antarctic coast ΔfCO₂(w–a) values of below –60 μatm were observed in a coastal polynya between 8° W and 0° W. In late December the southeastern Weddell Gyre

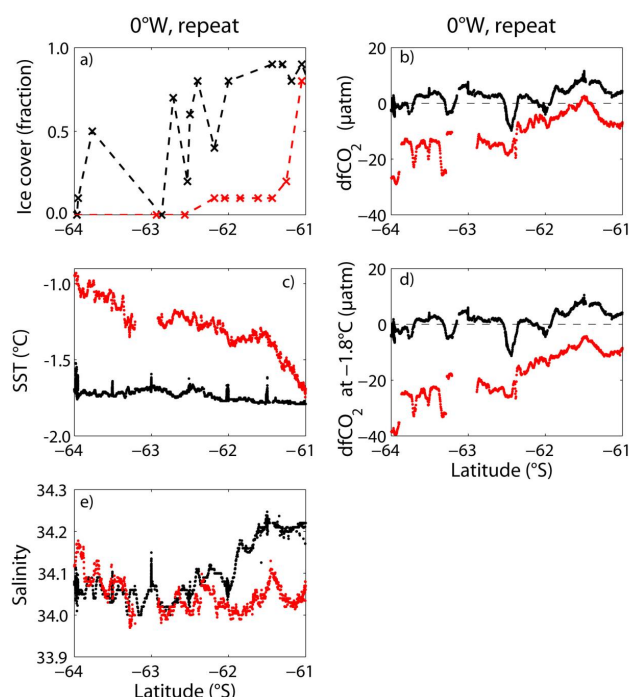


Fig. 4. (a) Sea ice cover (fraction), (b) the difference of fCO₂ across the sea surface, ΔfCO₂(w–a), (c) sea surface temperature, (d) ΔfCO₂(w–a) for fCO₂w corrected to –1.8°C, and (e) salinity on 8 to 10 December 2002 (black) and 20 December 2002 (red) for 61° S to 64° S along 0° W.

at 17° E to 23° E was in a rapid transition from ice cover to open water (Fig. 2b), while fCO₂ varied from slight to strong supersaturation. All sea ice had vanished by the time the ship sailed northwards north of 68.2° S 18.1° E on 3 January 2003. Within ice-free waters we observed undersaturation of fCO₂ and low DIC in phytoplankton blooms between 58.5° S and 62.5° S along 23° E.

3.2 The vertical distribution of temperature and DIC

Contour plots of potential temperature in the upper 400 m along 0° W and 17° E to 23° E show the temperature maximum of the WDW, a temperature minimum above it and a shallow, relatively warm surface layer, where sea ice melting and subsequent warming had occurred (Fig. 5a, b). The stations closest to Antarctica are in the westward flowing Antarctic Coastal Current. The WDW had several local temperature maxima between 1.2°C and 1.5°C along both sections. Along 17° E to 23° E the core of WDW was shallower in the south than further to the north (Fig. 5b), while this lateral variation was less pronounced along 0° W (Fig. 5a). Effects due to the vicinity of Maud Rise are apparent in the temperature profiles along 0° W between 63° S and 66° S (Fig. 5a). The WDW is characterised by high DIC along both sections (Fig. 6a, b). The DIC

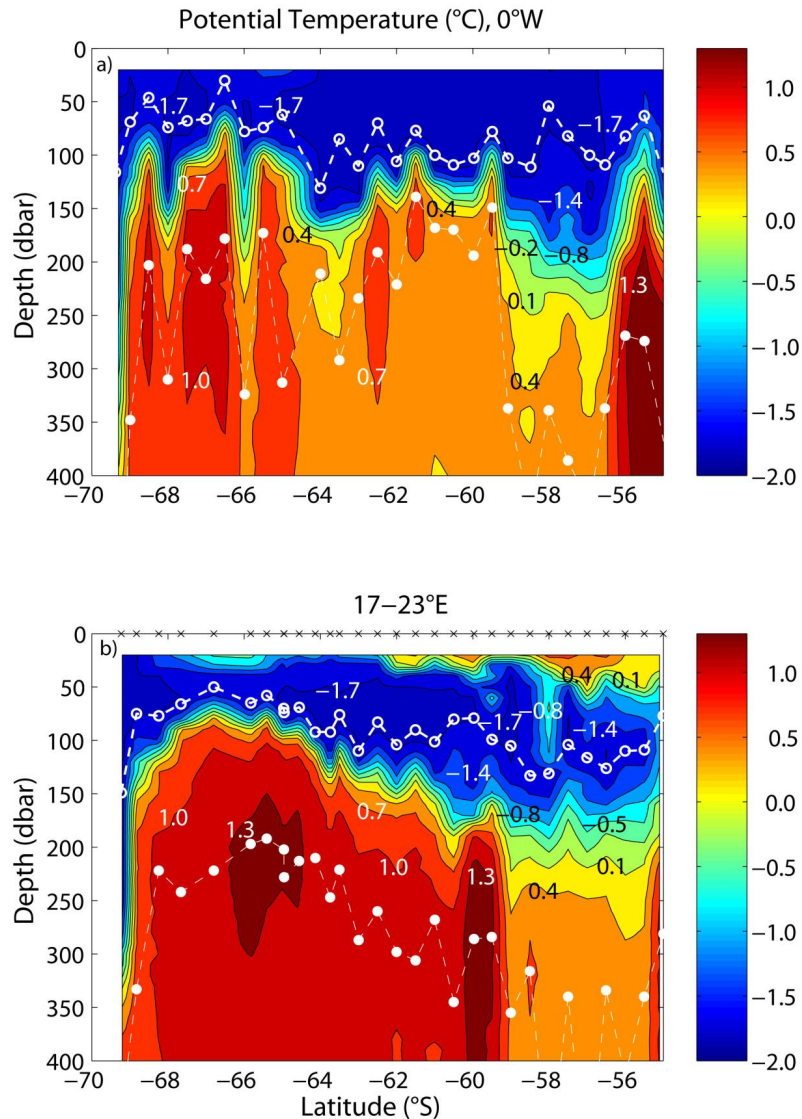


Fig. 5. Potential temperature in the upper 400 m (a) along 0° W, and (b) 17° E to 23° E with indication of the temperature minimum plus 0.02°C (open circles) and the temperature maximum (filled circles). Contours are at 0.3°C intervals.

maximum below 200 m depth between 59.0° S and 64.0° S along 0° W (Fig. 6a) is associated with Central Intermediate Water (CIW) (Whitworth and Nowlin, 1987; Hoppema et al., 1997).

A temperature minimum, a remnant of the winter mixed layer (WML), was evident above the pycnocline (Fig. 5a, b). The WML depth is defined here as the depth below the temperature minimum, where potential temperature exceeded the temperature minimum by 0.02°C (Figs. 5, 7a, b). This 0.02°C increment has little effect on the WML depth at most stations, but improves its identification at some stations. The temperature of the temperature minimum was higher in the southern Weddell Gyre (−1.7°C) than in the northern gyre (−1.8°C) (Fig. 7a) and was above the freezing

temperature of seawater at −1.88°C. This slight temperature excess of the WML reflects the introduction of heat from the WDW during winter (Gordon et al., 1984). Winter mixed layers depths were 30 to 80 m in the southern gyre (64.5° S to 69.0° S) and 50 to 130 m in the northern gyre (57.5° S to 64.0° S) along both sections (Fig. 7b). Stations at 66.8° S 17.0° E and 64.5° S 0° W had WML depths shallower than 50 m and high DIC at 50 m depth (Fig. 7b, c), possibly reflecting recent upward movement of WDW.

Here DIC at 50 m depth is taken to represent DIC in the WML, at least if the WML depth exceeded 50 m (Fig. 7b, c). Nonetheless spring-time processes had significantly reduced DIC at 50 m depth at stations where the WML depth exceeded 75 m, e.g. DIC was lower at 50 m than at 75 m depth

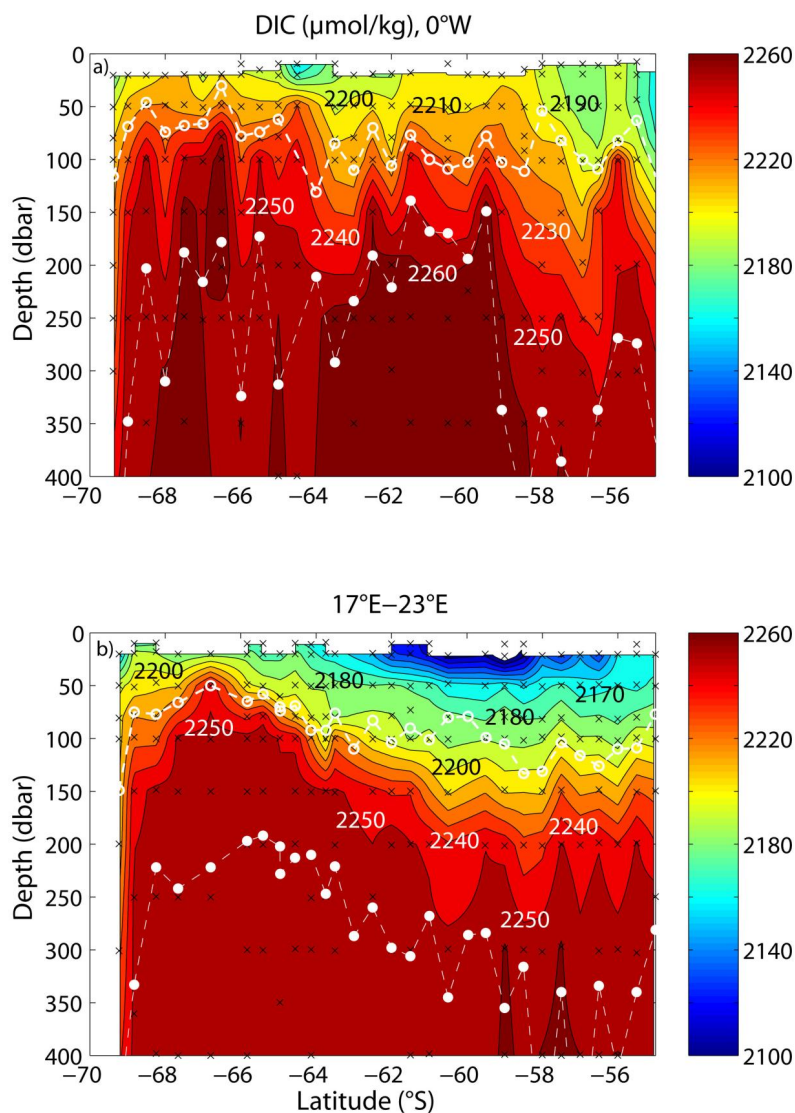


Fig. 6. The distribution of dissolved inorganic carbon (DIC) in the upper 400 m (a) along 0° W and (b) 17° E to 23° E with indication of the temperature minimum plus 0.02°C (open circles) and the temperature maximum (closed circles). Contours are at 10 $\mu\text{mol kg}^{-1}$ intervals. Crosses indicate sampling depths.

by 7.0 $\mu\text{mol kg}^{-1}$ (σ of 5.3 $\mu\text{mol kg}^{-1}$ for 10 data points) along 0° W and by 13.0 $\mu\text{mol kg}^{-1}$ (σ of 5.5 $\mu\text{mol kg}^{-1}$, n of 16) along 17° E to 23° E.

The DIC concentration at 50 m depth was higher by about 5 $\mu\text{mol kg}^{-1}$ in the southern Weddell Gyre than further north along 0° W, if the station with a shallow WML at 64.5° S is ignored (Fig. 7c). The northern Weddell Gyre along 23° E had low DIC and salinity in the upper 50 m. This freshening cannot be explained by melting of sea ice alone and could reflect the presence of waters with an ACC origin, since surface waters in the ACC have lower salinity than in the Weddell Gyre.

The DIC difference between 50 m and 20 m depth is used as a measure for changes in surface water DIC from winter to spring and summer (Fig. 8), while recognising that this may underestimate the seasonal changes in DIC. The DIC change due to ice melting and other fresh water inputs was calculated by correcting DIC at 50 m depth to the salinity at 20 m depth. The DIC change resulting from organic matter production was estimated from the change in nitrate from 50 m to 20 m, while assuming carbon to nitrogen uptake in a ratio of 117 moles to 16 moles (Anderson and Sarmiento, 1994). Residual DIC changes include the effects of CaCO₃ dissolution or precipitation and CO₂ air-sea exchange.

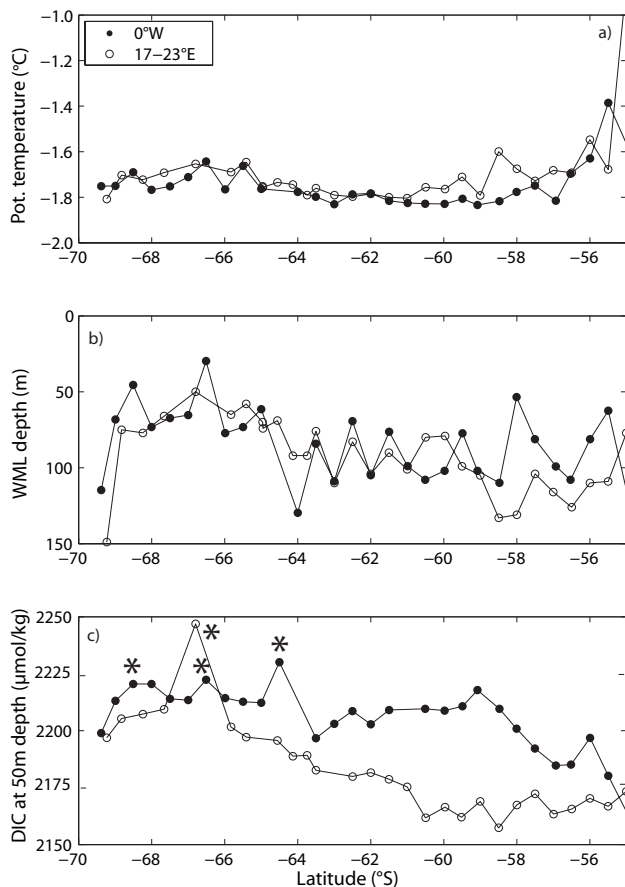


Fig. 7. (a) The potential temperature and (b) depth of the temperature minimum plus 0.02°C and (c) the DIC concentration at 50 m depth along 0° W and 17° E to 23° E. (b) The winter mixed layer (WML) depth is taken as the depth of the temperature minimum plus 0.02°C. (c) Star symbols indicate stations with a temperature minimum at or above 50 m depth.

Absolute DIC changes between 50 m and 20 m increased along the cruise track from 0° W to the eastern gyre (Fig. 8). The DIC changes were small north of 62° S along 0° W below heavy ice cover in early December. Ice melt and other freshwater inputs locally reduced surface water DIC by 20 $\mu\text{mol kg}^{-1}$ along 0° W and by 40 $\mu\text{mol kg}^{-1}$ along 17° E to 23° E. The inflow of surface water from the ACC may have contributed to the large DIC reduction in the northeastern gyre. Organic matter production decreased DIC by 40–60 $\mu\text{mol kg}^{-1}$ in phytoplankton blooms in a polynya at 64.5° S 0° W and in open water in the northeastern Weddell Gyre. Residual DIC changes ranged from –15 to 12 $\mu\text{mol kg}^{-1}$.

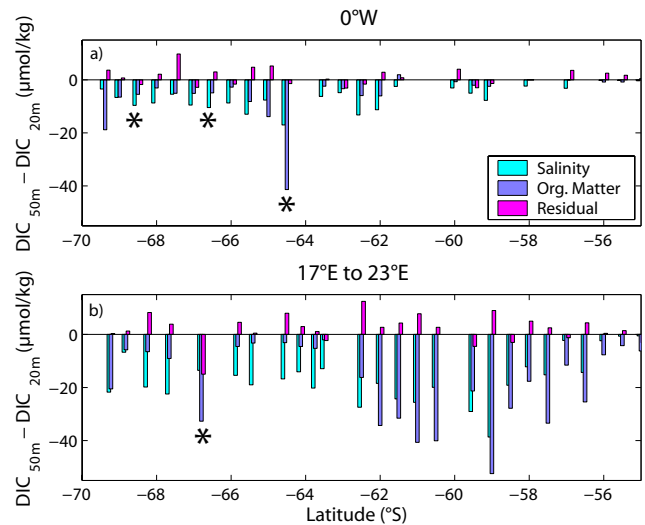


Fig. 8. The difference in the DIC concentration from 50 m to 20 m depth (a) for 0° W and (b) 17° E to 23° E. The changes are ascribed to freshwater inputs (denoted as “Salinity”), biological carbon uptake for organic matter production (denoted as “Org Matter”) and further processes (denoted as “Residual”), including CO₂ air-sea exchange and CaCO₃ precipitation or dissolution. Star symbols indicate stations with a temperature minimum at or above 50 m depth. The effect of biological carbon uptake has been calculated for a ratio of 117 moles of carbon to 16 moles of nitrate (Anderson and Sarmiento, 1994).

4 Discussion

4.1 Processes affecting CO₂ chemistry during and upon ice melt

The processes affecting CO₂ chemistry during and upon ice melt are further studied by comparing the behaviour of near-surface water fCO₂, DIC and calculated alkalinity along the cruise track (Fig. 9). The effect of ice melting on TA and DIC has been removed by normalisation to a salinity of 34.2, as this is usually done. Friis (personal communication) suggest that freshening of surface water may reduce fCO₂ by ~12 μatm per unit of salinity decrease. Here the change in salinity in surface waters by ice melt was less than 0.5 units in most of the Weddell Gyre and up to 1.5 units near 59° S 23° E (Fig. 3c). Thus, freshening may have reduced fCO₂ by 6 μatm and in the extreme case by up to 18 μatm .

Normalised DIC (DIC_{34.2}) and fCO₂ have a good correspondence. Normalised alkalinity (TA_{34.2}) has a range of 2305 to 2330 $\mu\text{mol kg}^{-1}$. Data for DIC_{34.2} and TA_{34.2} cluster together with a “tail” on the left (Fig. 9a). Tentatively lines with a slope of 2:1 have been drawn in the plots, with the purpose to explore changes in TA_{34.2} and DIC_{34.2}. The ratio of 2:1 corresponds to changes in TA_{34.2} and DIC_{34.2} by CaCO₃ precipitation or calcification (negative changes) and CaCO₃ dissolution (positive changes). For example, the right

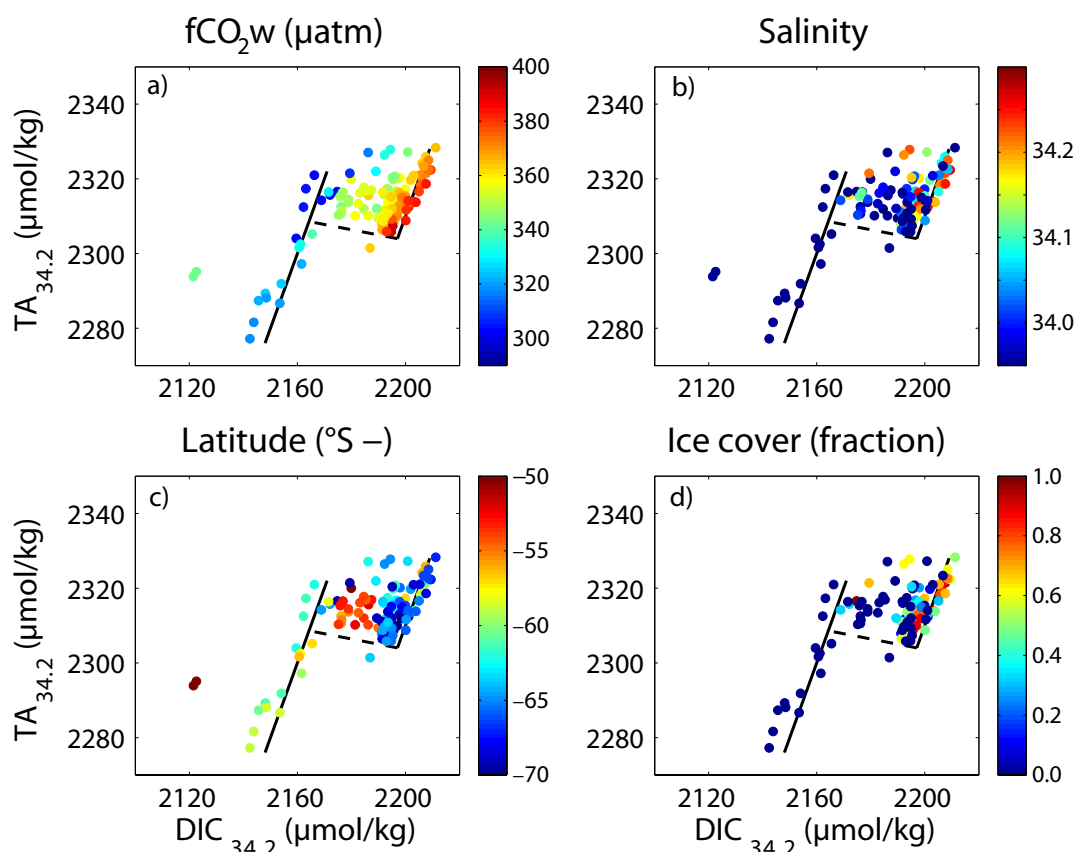


Fig. 9. Estimated alkalinity and DIC, both normalised to a salinity of 34.2, from 10 and 20 m depth (a) for surface water $f\text{CO}_2$, (b) salinity, (c) latitude, and (d) the shipboard observations of the sea ice cover interpolated to the timing of the CTD casts. The continuous lines correspond to theoretical changes in $\text{TA}_{34.2}$ and $\text{DIC}_{34.2}$ in a ratio of 2:1 by precipitation and dissolution of CaCO_3 , while the dashed line indicates the effect of organic matter production and remineralisation at a ratio for $\text{TA}_{34.2}$ to $\text{DIC}_{34.2}$ of $-0.14:1$ (Anderson and Sarmiento, 1994).

line corresponds to increases in $\text{TA}_{34.2}$ and $\text{DIC}_{34.2}$ of 24 and $12 \mu\text{mol kg}^{-1}$, resulting in a decrease of $f\text{CO}_2$ by $27 \mu\text{atm}$. Most stations with dense sea ice cover and high surface salinity are close to the right line (Fig. 9b, d). Points near the right line include the non-bloom stations along 0°W , some data from the cross-section and stations south of 64°S in the eastern gyre.

Organic matter production changes DIC and TA in a ratio of -1 to $+0.14$ (Anderson and Sarmiento, 1994), as shown by the dashed line (Fig. 9a). The line corresponds to changes in $\text{DIC}_{34.2}$ by $-33 \mu\text{mol kg}^{-1}$, in $f\text{CO}_2$ by $-90 \mu\text{atm}$ and in $\text{TA}_{34.2}$ by $4.6 \mu\text{mol kg}^{-1}$. The bloom stations at 0°W appear to the left of the right line, almost certainly reflecting organic matter production during and upon ice melt.

Data close to the lower left line (or “tail”) with a 2:1 slope (Fig. 9a) are from surface waters between 58.5°S and 62.5°S along 23°E , which have low $\text{TA}_{34.2}$ and $\text{DIC}_{34.2}$, a possible ACC origin and are home to an intense phytoplankton bloom. Along the tail surface water $f\text{CO}_2$ increases by $38 \mu\text{atm}$ for decreases in $\text{TA}_{34.2}$ and $\text{DIC}_{34.2}$ of 46 and $23 \mu\text{mol kg}^{-1}$, respectively.

The tentative 2:1 slope describes the data fairly well, but is an approximation. Below the origin of the approximate 2:1 slope of the two lines is investigated. First the potential effect of CaCO_3 dissolution on near surface alkalinity and DIC is assessed. Dieckman et al. (2008) report 0.3 to $3.0 \text{ g ikaite m}^{-2}$ sea ice in 0.30 m deep ice cores, or 1.4 to $14.4 \text{ mmol ikaite m}^{-2}$. In ANT XX/2 sea ice mostly consisted of first year ice with a thickness 0.3 to 1.2 m (Klatt, O., personal communication), but some ice melt might have occurred before our arrival. Here we assume an initial sea ice thickness of 1 m, $\text{TA}_{34.2}$ of $2310 \mu\text{mol kg}^{-1}$ and $\text{DIC}_{34.2}$ of $2200 \mu\text{mol kg}^{-1}$. Dissolution of ikaite in the ice into a 20 m deep surface layer would change $\text{TA}_{34.2}$ by 0.4 to $4.5 \mu\text{mol kg}^{-1}$, $\text{DIC}_{34.2}$ by 0.2 to $2.2 \mu\text{mol kg}^{-1}$ and $f\text{CO}_2$ by -0.5 to $-5.0 \mu\text{atm}$. Thus, the maximum effect of ikaite dissolution for rapid melting of sea ice in a shallow surface layer is small. However, higher ikaite concentrations have been found elsewhere (Dieckmann, G., personal communication). It is therefore still possible that the tentative 2:1 slope of the right line (Fig. 9a) results from CaCO_3 processes in sea ice. Future research is needed to properly investigate

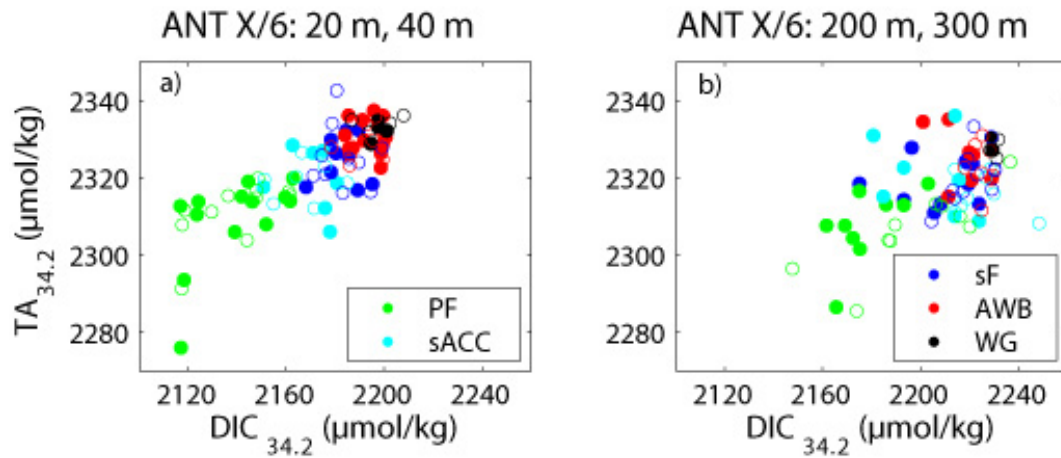


Fig. 10. Normalised alkalinity and DIC for (a) 20 m, 40 m, (b) 200 m and 300 m depth along 6° W from ANT X/6 (data from Rommets et al., 1997). Both TA and DIC were normalised to a salinity of 34.2. The symbols correspond to depths of (a) 20 m (filled circles), 40 m (open circles), (b) 200 m (filled circles) and 300 m (open circles). The colours indicate hydrographic regions (Bakker et al., 1997), notably the Polar Frontal region (PF, 46.8° S to 50.8° S), the southern ACC (sACC, 50.8° S to 54.3° S), the southern Front (SF, 54.3° S to 56.3° S), the ACC-Weddell Gyre Boundary (AWB, 56.3° S to 58.8° S) and the Weddell Gyre (WG, 58.8° S to 59.9° S).

the effect of CaCO₃ precipitation and dissolution on the CO₂ chemistry of brines and surface water during ice formation and sea ice melt.

One obvious hypothesis for the approximate 2:1 slope of the left line or “tail” (Fig. 9a) is strong calcification in the phytoplankton bloom at 23° E. However, this does not account for sizeable DIC uptake by organic matter production, as suggested by the nitrate reduction from 50 m to 20 m depth (Fig. 8b), which would have strongly changed the slope. Also observations of calcifying phytoplankton this far south are rare (Thomsen et al., 1988; Winter et al., 1999).

The origin of the 2:1 slopes was further investigated for measurements of TA and DIC between 47° S and 60° S along 6° W during *Polarstern* cruise ANT X/6 in October and November 1992 (Bakker et al., 1997; Rommets et al., 1997). The transect extended from the ACC (46.8° S to 56.3° S), to the ACC-Weddell Gyre Boundary (AWB) (56.3° S to 58.8° S), and the northern Weddell Gyre (58.8° S to 59.8° S) in a period with rapidly melting sea ice (Bakker et al., 1997). The data from ANT X/6 highlight a decrease of DIC_{34.2} from 300 m to 20 m depth at relatively constant TA_{34.2} (Fig. 10a, b), pointing to the impact of organic matter production and remineralisation on DIC_{34.2}. Normalised alkalinity displays a north-south gradient of $\sim 40 \mu\text{mol kg}^{-1}$ in the upper 300 m with on average lower values in the ACC than further south near the AWB and in the northern Weddell Gyre (Fig. 10a, b). We infer that upwelling of CDW (in the ACC) and WDW (in the Weddell Gyre) transfers the north-south gradient in TA_{34.2} at depth to the surface ocean. Likewise variable TA_{34.2} in upwelled water may cause some variation of TA_{34.2} in Weddell Gyre surface waters.

4.2 Ice covered CO₂-rich waters

High values of surface water fCO₂ and DIC were found below the sea ice in late spring in the Weddell Gyre (Fig. 3). Upward movement and entrainment of DIC-rich WDW into the winter mixed layer contributed strongly to these high values. Temperatures and DIC were higher at the temperature minimum, while winter mixed layers were shallower, in the southern than in the northern gyre (Fig. 7a–c). This suggests that the upward movement and entrainment of WDW into the winter mixed layer were stronger in the southern gyre than further north, both along 17° E to 23° E and along 0° W, as was previously suggested for waters near 0° W (Gordon and Huber, 1990). It is likely that upward movement and entrainment of WDW into the mixed layer continued below the sea ice, at least while air temperatures were cold enough to remove the heat from the WDW input (Gordon and Huber, 1990).

While the ice and leads in the ice would have allowed heat to escape from the winter mixed layer to the atmosphere, the ice cover would have prevented major release of CO₂ and other gases, which is evidenced by major under- or supersaturation of gases under the ice cover (Gordon et al., 1984; Klatt et al., 2002). Factors contributing to this are that only insignificant gas exchange occurs through the ice itself (but see, e.g. Anderson et al., 2004), and ice reduces the fetch of the wind and the gas transfer velocity for leads in the ice. And even in non-ice covered waters dissolved CO₂ takes many months to reach equilibrium with the atmospheric CO₂ content by air-sea gas exchange, as a consequence of the large carbonate buffer in seawater. The bottom line is that we expect supersaturation of CO₂ under the sea-ice pack due

to upwelling and entrainment of WDW into the winter mixed layer, in agreement with our measurements and with earlier observations in the wintertime Weddell Gyre (Weiss et al., 1992).

4.3 From ice covered CO₂-rich waters to a biologically mediated CO₂ sink

Ice melting first occurred northwest of Maud Rise in the first half of December 2002, creating a transient polynya (Fig. 2). Relatively early ice melting at 60° S to 61° S and 66° S to 67° S along 17° E to 23° E in mid-December coincided with the presence of warm WDW cores below the winter mixed layer (Figs. 2, 5b). Ice melting itself reduced surface water DIC by up to 40 μmol kg⁻¹ through dilution (Fig. 8). During and upon ice melting, net community production rapidly reduced fCO₂ and DIC by up to 100 μatm and 60 μmol kg⁻¹, respectively (Figs. 3, 8), thus converting a potential oceanic CO₂ source into a sink for atmospheric CO₂. This reduction of fCO₂ from supersaturation to undersaturation already started during ice melt, as is shown by fCO₂ close to the atmospheric value on the repeat section along 0° W on 8 to 10 December (Fig. 4). Zemmeling et al. (2008) have demonstrated that biological activity occurs in leads in Weddell Sea ice in early spring.

Sea ice in regions with ice melt frequently had a brown layer of about 5 cm thick, indicative of ice algae, somewhat above the ice-water interface. It is probable that the ice algae had taken up DIC from the surrounding brine and that mixing in of this brine contributed to the rapid reduction of surface water fCO₂ and DIC during ice melt. We have found no direct evidence of the effects of CaCO₃ processes in sea ice on CO₂ chemistry in surface water (Fig. 9). Surface water fCO₂ decreased at a rate of 1.0 to 2.5 μatm d⁻¹ in a phytoplankton bloom on the repeat section at 0° W (Fig. 4). Since surface water fCO₂ was close to the atmospheric CO₂ value during our first visit, biological CO₂ uptake for 11 days sufficed to create a small CO₂ sink, by which time the ice had almost completely disappeared.

Our observations of high wintertime CO₂ values below the ice with rapid transition to a biologically-mediated CO₂ sink during and upon ice melt fit well with other data from the region. Notably supersaturation of fCO₂ by 0 to 40 μatm was determined in the southeastern Weddell Gyre in June–November 1986 during ANT V/2 and V/3 (Weiss et al., 1992), while strong undersaturation of fCO₂ by 60 to 130 μatm, was found along the Prime Meridian in January to February 1984 during Ajax 2 (Weiss et al., 1992).

Past cruises along 0° W hint at an opposite shift from fCO₂ undersaturation to supersaturation in autumn. In April 1996 modest supersaturation by 10 μatm and undersaturation by 15 μatm were observed north and south of about 60° S, respectively (Hoppema et al., 2000). By contrast, in April to May 1998 surface water fCO₂ was supersaturated by 20 to 30 μatm south of 64° S, while mixed layers were signifi-

cantly deeper and more saline in autumn 1998 than in April 1996 (Bellerby et al., 2004). This suggested that (more) entrainment of WDW into the mixed layer had occurred in 1998 than in 1996 (Bellerby et al., 2004). Further north fCO₂ was similar in autumn 1996 and 1998. High fCO₂ values in autumn before the formation of the sea ice pack would provide a short window for CO₂ outgassing to the atmosphere.

Thus, high biological carbon uptake during and upon melting of the sea ice in late spring and summer creates a seasonal and annual CO₂ sink, as ice impedes outgassing of CO₂ from upwelled CO₂-rich waters below the winter ice. It is possible that dissolution of CaCO₃ during ice melt plays a minor role in the reduction of fCO₂. These findings are in agreement with the Weddell Sea as a CO₂ sink (Hoppema et al., 1999; Stoll et al., 1999). A similar mechanism has been proposed for the seasonally ice-covered Northeast Water Polynya off Greenland (Yager et al., 1995), where waters below the winter ice are supersaturated in CO₂ due to strong remineralisation of organic matter, but where rapid biological carbon uptake creates an annual CO₂ sink upon melting of the sea ice.

The modern Weddell Gyre CO₂ sink is thus preconditioned by upwelling of CO₂-charged WDW and rapid biological carbon uptake during and upon ice melt. In pre-industrial times the relative CO₂ source from the upwelled water would have been stronger by about 100 μatm, thus creating an overall, annual CO₂ source (Hoppema, 2004) with biologically mediated, summertime supersaturation of surface water fCO₂ by 50 μatm, assuming that biological carbon uptake did not change much.

Gordon and Huber (1990) estimated the residence time of Weddell Sea surface water as 2.5 years, based on an average annual upwelling of WDW of 45 m close to the Prime Meridian with higher upwelling of 50 to 75 m in the southern gyre. Hoppema et al. (1995) derived an annual upwelling of 30 m for the western Weddell Gyre at 65° S 40° W. Surface water leaves the Weddell Gyre as surface water flowing into the ACC along the northern boundary of the gyre or as AABW, which is formed along the southern and southwestern margins of the gyre. The above suggests that upwelled WDW in the southern Weddell Gyre, with its high upwelling rates and short ice free periods (5 months per year), has little opportunity for exchanging gases with the atmosphere, before some of it becomes part of AABW. This fits well with observations of low CFC concentrations in the surface water source of AABW (Klatt et al., 2002) and estimates of a low anthropogenic CO₂ content in AABW (Poisson and Chen, 1987; Hoppema et al., 2001).

Upwelling of CO₂-enriched deep water also occurs elsewhere around Antarctica, which is indicated by the distribution of oxygen. Oxygen (O₂) at 100 m depth shows a distinct minimum between 65° S and 69° S in the eastern and central Weddell Gyre (Olbers et al., 1992; unpublished results from ANT XX/2), reflecting the upwelling of O₂-poor (and CO₂-rich) WDW. The O₂ minimum is particularly deep at 10° W

to 10° E and extends into the western gyre (Olbers et al., 1992). A similar O₂ minimum is found in a discontinuous, circumpolar band around Antarctica, which suggests that upwelling of CDW at a short distance off Antarctica also occurs in the ACC, rather than in the Weddell Gyre alone. It remains to be seen whether seasonal sea ice coverage and rapid summertime biological carbon uptake equally prevent ventilation of the CO₂ from this discontinuous ring of upwelled CDW around Antarctica.

Our observations of a rapid transition from ice-covered CO₂-rich waters to a biologically mediated CO₂ sink during and upon ice melt support the hypothesis by Stephens and Keeling (2000) that more winter-time sea ice cover in glacial periods would have reduced wintertime ventilation of CO₂ in the Southern Ocean, thus contributing to the observed decrease in atmospheric CO₂. Even if the Antarctic sea ice would have melted back in glacial summer, rapid biological CO₂ uptake during and upon ice melt would have strongly reduced outgassing of CO₂.

5 Conclusions

The observations demonstrate high DIC in the winter mixed layer by upwelling and entrainment of WDW in the eastern Weddell Gyre. Seasonal sea ice cover prevents outgassing from these CO₂-rich waters. Rapid biological CO₂ uptake during and upon ice melt creates a summertime CO₂ sink. Despite the tendency of the surfacing of WDW to cause CO₂ supersaturation, the Weddell Gyre may well be a CO₂ sink on an annual basis due to this effective fCO₂ reduction mechanism, as suggested by Hoppema (2004). The CO₂ source tendency deriving from the upward movement of 'pre-industrial' CDW is currently declining, as atmospheric CO₂ levels continue to increase. Thus, the CO₂ sink of the Weddell Gyre will continue to increase (provided the upward movement of WDW does not change much). Our observations seem to support the hypothesis that an increase in sea ice coverage contributed to the decrease of atmospheric CO₂ in glacial periods (Stephens and Keeling, 2000).

Acknowledgements. We are grateful to the captain and crew of FS *Polarstern* and chief scientist D. Fütterer for a memorable cruise. O. Klatt (AWI) directed the shipboard ice observations, to which many scientists on board contributed. We thank E. Fahrbach (AWI) and Y. Bozec (formerly at the Royal Netherlands Institute for Sea Research) for providing pre-cruise support and A. Wisotzki (AWI) for making the ice maps. J. Bendtsen (Natural Environmental Research Institute, Denmark), K. Friis and two anonymous reviewers provided thoughtful comments. The Royal Society (JEB/15221) and the CARBOOCEAN (GOCE-511176-1) and CASIX (Centre for Observations of Air-Sea Interactions and Fluxes, NER/F14/G6/115) projects provided funding for the research. The Alfred Wegener Institute is gratefully acknowledged for hosting D. C. E. Bakker as a guest scientist.

Edited by: J.-P. Gattuso

References

- Anderson, L. A. and Sarmiento, J. L.: Redfield ratios of remineralization determined by nutrient data analysis, *Global Biogeochem. Cy.*, 8, 65–80, 1994.
- Anderson, L. G., Falck, E., Jones, E. P., Jutterström, S., and Swift, J. H.: Enhanced uptake of atmospheric CO₂ during freezing of seawater: A field study in Storfjorden, Svalbard, *J. Geophys. Res.*, 109, C06004, doi:10.1029/2003JC002120, 2004.
- Bagriantsev, N. V., Gordon, A. L., and Huber, B. A.: Weddell Gyre: Temperature maximum stratum, *J. Geophys. Res.*, 94, 8331–8334, 1989.
- Bakker, D. C. E., De Baar, H. J. W., and Bathmann, U. V.: Changes of carbon dioxide in surface waters during spring in the Southern Ocean, *Deep-Sea Res. II*, 44, 91–127, 1997.
- Bakker, D. C. E., De Baar, H. J. W., and De Jong, E.: The dependence on temperature and salinity of dissolved inorganic carbon in East Atlantic surface waters, *Mar. Chem.*, 65, 263–280, 1999.
- Bakker, D. C. E., Watson, A. J., and Law, C. S.: Southern Ocean iron enrichment promotes inorganic carbon drawdown, *Deep-Sea Res. II*, 48, 2483–2507, 2001.
- Bellerby, R. G. J., Hoppema, M., Fahrbach, E., De Baar, H. J. W., and Stoll, M. H. C.: Interannual controls on Weddell Sea surface water fCO₂ during the autumn-winter transition phase, *Deep-Sea Res. I*, 51, 793–808, 2004.
- Carmack, E. C. and Foster, T. D.: On the flow of water out of the Weddell Sea, *Deep-Sea Res.*, 22, 711–724, 1975.
- Comiso, J.: Bootstrap sea ice concentrations from NIMBUS-7 SMMR and DMSP SSM/I, National Snow and Ice Data Center, Boulder, Colorado, USA, 1999, updated 2007.
- Deacon, G. E. R.: The Weddell Gyre, *Deep-Sea Res.*, 26A, 981–995, 1979.
- Dickson, A. G. and Millero, F. J.: A comparison of the equilibrium constants for the dissociation of carbonic acid in seawater media, *Deep-Sea Res.*, 34, 1733–1743, 1987.
- Dickson, A. G., Sabine, C. L., and Christian, J. R.: Guide to best practices for ocean CO₂ measurements. PICES special publication 3, 191 pp., 2007.
- Dieckmann, G. S., Nehrke, G., Papadimitriou, S., Göttlicher, J., Steininger, R., Kennedy, H., Wolf-Gladrow, D., and Thomas, D. N.: Calcium carbonate as ikaite crystals in Antarctic sea ice, *Geophys. Res. Lett.*, 25, L08501, doi:10.1029/2008GL033540, 2008.
- ETOPO 5: Digital relief of the surface of the earth, Data Announcement 88-MGG-02, NOAA, Natl. Geophys. Data Center, Boulder, Colorado, USA, 1988.
- Friis, K., Körtzinger, A., and Wallace, D. W. R.: The salinity normalization of marine inorganic carbon chemistry data, *Geophys. Res. Lett.*, 30, 1085–1088, 2003.
- Fütterer, D. K. and Kattner, G.: The Expedition ANTARKTIS-XX of RV "Polarstern" in 2002/2003, *Berichte zur Polar- und Meeresforschung*, 495, 1–106, 2005.
- Geibert, W., Rutgers van der Loeff, M. M., Hanfland, C., and Dauelsberg, H.-J.: Actinium-227 as a deep-sea tracer: Sources, distribution and applications, *Earth Planet. Sc. Lett.*, 198, 147–165, 2002.
- Gordon, A. L. and Huber, B. A.: Southern Ocean winter mixed layer, *J. Geophys. Res.*, 95, 11 655–11 672, 1990.
- Gordon, A. L., Chen, C. T. A., and Metcalf, W. G.: Winter mixed layer entrainment of Weddell Deep Water, *J. Geophys. Res.*, 89,

- 637–640, 1984.
- Gordon, A. L., Huber, B. A., Hellmer, H. H., and Field, A.: Deep and bottom water of the Weddell Sea's western rim, *Science*, 262, 95–97, 1993.
- Gouretski, V. V. and Danilov, A. I.: Weddell Gyre: Structure of the eastern boundary, *Deep-Sea Res. I*, 40, 561–582, 1993.
- Hoppema, M.: Weddell Sea turned from source to sink for atmospheric CO₂ between pre-industrial time and present, *Global Planet. Change*, 40, 219–231, 2004.
- Hoppema, M., Fahrbach, E., and Schröder, M.: On the total carbon dioxide and oxygen signature of the Circumpolar Deep Water in the Weddell Gyre, *Oceanol. Acta*, 20, 783–798, 1997.
- Hoppema, M., Fahrbach, E., Schröder, M., Wisotzki, A., and De Baar, H. J. W.: Winter-summer differences of carbon dioxide and oxygen in the Weddell Sea surface layer, *Mar. Chem.*, 51, 177–192, 1995.
- Hoppema, M., Fahrbach, E., Stoll, M. H. C., and De Baar, H. J. W.: Annual uptake of atmospheric CO₂ by the Weddell Sea derived from a surface layer balance, including estimations of entrainment and new production, *J. Mar. Systems*, 19, 219–233, 1999.
- Hoppema, M., Roether, W., Bellerby, R. G. J., and De Baar, H. J. W.: Direct measurements reveal insignificant storage of anthropogenic CO₂ in the abyssal Weddell Sea, *Geophys. Res. Lett.*, 28, 1747–1750, 2001.
- Hoppema, M., Stoll, M. H. C., and De Baar, H. J. W.: CO₂ in the Weddell Gyre and Antarctic Circumpolar Current: Austral autumn and early winter, *Mar. Chem.*, 72, 203–220, 2000.
- Jones, E. P. and Coote, A. R.: Oceanic CO₂ produced by the precipitation of CaCO₃ from brines in sea ice, *J. Geophys. Res.*, 86, 11 041–11 043, 1981.
- Klatt, O., Roether, W., Hoppema, M., Bultsiewicz, K., Fleischmann, U., Rodehacke, C., Fahrbach, E., Weiss, R. F., and Bullister, J. L.: Repeated CFC sections at the Greenwich Meridian in the Weddell Sea, *J. Geophys. Res.*, 107, 3030, doi:10.1029/2000JC000731, 2002.
- Le Quéré, C. L., Rödenbeck, C., Buitenhuis, E. T., Conway, T. J., Langenfelds, R., Gomez, A., Labuschagne, C., Ramonet, M., Nakazawa, T., Metzl, N., Gillett, N., and Heimann, M.: Saturation of the Southern Ocean CO₂ sink due to recent climate change, *Science*, 316, 1735–1738, 2007.
- Lenton, A. and Matear, R. J.: Role of the Southern Annular Mode (SAM) in Southern Ocean CO₂ uptake, *Global Biogeochem. Cy.*, 21, GB2016, doi:10.1029/2006GB002714, 2007.
- Lovenduski, N. S., Gruber, N., Doney, S. C., and Lima, I. D.: Enhanced CO₂ outgassing in the Southern Ocean from a positive phase of the Southern Annular Mode, *Global Biogeochem. Cy.*, 21, GB2026, doi:10.1029/2006GB002900, 2007.
- Martinson, D. G., Killworth, P. D., and Gordon, A. L.: A convective model for the Weddell Polynya, *J. Phys. Oceanogr.*, 11, 466–488, 1981.
- McNeil, B. I., Metzl, N., Key, R. M., Matear, R. J., and Corbière, A.: An empirical estimate of the Southern Ocean air-sea CO₂ flux, *Global Biogeochem. Cy.*, 21, GB3011, doi:10.1029/2007GB002991, 2007.
- Mehrbach, C., Culbertson, C. H., Hawley, J. E., and Pytkowicz, R. M.: Measurement of the apparent dissociation constants of carbonic acid in seawater at atmospheric pressure, *Limnol. Oceanogr.*, 18, 897–907, 1973.
- Millero, F. J.: Thermodynamics of the carbon dioxide system in seawater, *Geochim. Cosmochim. Ac.*, 59, 661–677, 1995.
- Moore, J. K. and Abbott, M. R.: Phytoplankton chlorophyll distributions and primary production in the Southern Ocean, *J. Geophys. Res.*, 105, 28 709–28 722, 2000.
- Muench, R. D., Morison, J. H., Padman, L., Martinson, D., Schlosser, P., Huber, B., and Hohmann, R.: Maud Rise revisited, *J. Geophys. Res.*, 106, 2423–2440, 2001.
- Odate, T., Furuya, K., and Fukuchi, M.: Photosynthetic oxygen production and community respiration in the Indian sector of the Antarctic Ocean during austral summer, *Polar Biol.*, 25, 859–864, 2002.
- Olbers, D., Gouretski, V., Seiss, G., and Schröder, J.: Hydrographic Atlas of the Southern Ocean, Alfred Wegener Institute, Bremerhaven, 1992.
- Orsi, A. H., Whitworth III, T., and Nowlin Jr., W. D.: On the meridional extent and fronts of the Antarctic Circumpolar Current, *Deep-Sea Res. I*, 42, 641–673, 1995.
- Papadimitriou, S., Kennedy, H., Kattner, G., Dieckman, G. S., and Thomas, D. N.: Experimental evidence for carbonate precipitation and CO₂ degassing during sea ice formation, *Geochim. Cosmochim. Ac.*, 63, 1305–1318, 2004.
- Papadimitriou, S., Thomas, D. N., and Kennedy, H.: Biogeochemical composition of natural sea ice brines from the Weddell Sea during early austral summer, *Limnol. Oceanogr.*, 58, 1809–1823, 2007.
- Poisson, A. and Chen, C.-T. A.: Why is there little anthropogenic CO₂ in the Antarctic Bottom Water?, *Deep-Sea Res.*, 34, 1255–1275, 1987.
- Rommets, J. W., Stoll, M. H. C., De Koster, R. X., De Bruin, T. F., De Baar, H. J. W., Bathmann, U. V., and Smetacek, V.: R. V. Polarstern cruise ANT X/6, Cruise Database, *Deep-Sea Res. II*, 44, CD-ROM Appendix, 1997.
- Rysgaard, S., Glud, R. N., Sejr, M. K., Bendtsen, J., and Christensen, P. B.: Inorganic carbon transport during sea ice growth and decay: A carbon pump in polar seas, *J. Geophys. Res.*, 112, C03016, doi:10.1029/2006JC003572, 2007.
- Sabine, C. L., Feely, R. A., Gruber, N., Key, R. M., Lee, K., Bullister, J. L., Wanninkhof, R., Wong, C. S., Wallace, D. W. R., Tilbrook, B., Millero, F. J., Peng, T.-H., Kozyr, A., Ono, T., and Rios, A. F.: The oceanic sink for anthropogenic CO₂, *Science*, 305, 367–371, 2004.
- Schlitzer, R.: Carbon export fluxes in the Southern Ocean: results from inverse modeling and comparison with satellite-based estimates, *Deep-Sea Res. II*, 49, 1623–1644, 2002.
- Schröder, M. and Fahrbach, E.: On the structure and the transport of the eastern Weddell Gyre, *Deep-Sea Res. II*, 46, 501–527, 1999.
- Smith, W. H. F. and Sandwell, D. T.: Global sea floor topography from satellite altimetry and ship depth soundings, *Science*, 277, 1956–1962, 1997.
- Stephens, B. B. and Keeling, R. F.: The influence of Antarctic sea ice on glacial-interglacial CO₂ variations, *Nature*, 404, 171–174, 2000.
- Stoll, M. H. C., De Baar, H. J. W., Hoppema, M., and Fahrbach, E.: New early winter fCO₂ data reveal continuous uptake of CO₂ by the Weddell Sea, *Tellus*, 51B, 679–687, 1999.
- Sullivan, C. W., Arrigo, K. R., McClain, C. R., Comiso, J. C., and Firestone, J.: Distributions of phytoplankton blooms in the Southern Ocean, *Science*, 262, 1832–1837, 1993.
- Thomsen, H. A., Buck, K. R., Coale, S. L., Garrison, D. L., and

- Gowing, M. M.: Nanoplanktonic coccolithophorids (Prymnesiophyceae, Haptophyceae) from the Weddell Sea, Antarctica, *Nord. J. Bot.*, 8, 419–436, 1988.
- Tynan, C. T.: Ecological importance of the Southern Boundary of the Antarctic Circumpolar Current, *Nature*, 392, 708–710, 1998.
- Usbeck, R.: Modeling of marine biogeochemical cycles with an emphasis on vertical particle fluxes, Ph. D. thesis, Alfred Wegener Institute, Bremerhaven, *Berichte zur Polarforschung*, 332, 1–105, 1999.
- Wanninkhof, R. and Thoning, K.: Measurement of fugacity of CO₂ in surface water using continuous and discrete sampling methods, *Mar. Chem.*, 44, 189–205, 1993.
- Weiss, R. F., Van Woy, F. A., and Salameh, P. K.: Surface water and atmospheric carbon dioxide and nitrous oxide observations by shipboard automated gas chromatography: Results from expeditions between 1977 and 1990, *Scripps Inst. of Oceanogr. Ref. 92-11, ORNL/CDIAC-59, NDP-044, Carbon Dioxide Information Analysis Center*, 144 pp., 1992.
- Whitworth III, T. and Nowlin Jr., W. D.: Water masses and currents of the Southern Ocean at the Greenwich Meridian, *J. Geophys. Res.*, 92, 6462–6476, 1987.
- Winter, A., Elbrachter, M., and Krause, G.: Subtropical coccolithophorids in the Weddell Sea, *Deep-Sea Res. I*, 46, 439–449, 1999.
- Worby, A., Allison, I., and Dirita, V.: A technique for making ship-based observations of Antarctic sea ice thickness and characteristics. Part I Observational technique and results, Part II User operating manual, Antarctic CRC, Res. rep. 14, 63 pp., 1999.
- Yager, P. L., Wallace, D. W. R., Johnson, K. M., Smith Jr., W. O., Minnett, P. J., and Deming, J. W.: The Northeast water polynya as an atmospheric CO₂ sink: A seasonal rectification hypothesis, *J. Geophys. Res.*, 100, 4389–4398, 1995.
- Zemmelink, H. J., Houghton, L., Dacey, J. W. H., Stefels, J., Koch, B. P., Schröder, M., Wisotzki, A., Scheltz, A., Thomas, D. N., Papadimitriou, S., Kennedy, H., Kuosa, H., and Dittmar, T.: Stratification and the distribution of phytoplankton, nutrients, inorganic carbon and sulfur in the surface waters of Weddell Sea leads, *Deep-Sea Res. II*, 55, 988–999, 2008.
- Zickfeld, K., Fyfe, J. C., Saenko, O. A., Eby, M., and Weaver, A. J.: Response of the global carbon cycle to human-induced changes in Southern Hemisphere winds, *Geophys. Res. Lett.*, 34, L12712, doi:10.1029/2006GL028797, 2007.